Impact Welding Structural Aluminium Alloys to High Strength Steels Using Vaporizing Foil Actuator

B. Liu*, A. Vivek, G. S. Daehn

Department of Materials Science and Engineering, The Ohio State University, USA
*Corresponding author. Email: liu.2004@osu.edu

Abstract

Dissimilar Al/Fe joining was achieved using vaporizing foil actuator welding. Flyer velocities up to 727 m/s were reached using 10 kJ input energy. Four Al/Fe combinations involving AA5052, AA6111-T4, JAC980, and JSC1500 were examined. Weld samples were mechanically tested in lap-shear in three conditions: as-welded, corrosion-tested with e-coating, and corrosion-tested without coating. In all three conditions, the majority of the samples failed in the base aluminium instead of the weld. This shows that the weld was stronger than at least one of the base materials, both before and after corrosion testing. Galvanic corrosion was not significant since the differences in open cell potential, which represent the driving forces for galvanic corrosion, were small among these materials—no more than 60 mV in all cases. Nonetheless, through corrosion testing, the base materials suffered general corrosion, which accounted for the weakening of the base materials.

Keywords

Vaporizing foil actuator welding, Ultra-high strength steel, Aluminium

1 Introduction

Vehicle lightweighting has been a major push among automakers, largely due to increasing cost of energy and aggressive fuel efficiency goals (Joost, 2012). Conventional car bodies are mainly made of steel, but their weight can be reduced by substituting components of the car body for materials that provide higher specific strengths, such as structural aluminium alloys and high-strength steels. However, the incorporation of these materials calls for effective joining techniques, and since these materials are often drastically

different from one another, joining them together is often a nontrivial task. Fusion-based welding such as resistance spot welding, which is most common in automotive manufacturing, is usually not suitable for dissimilar joining due to melting point disparities between materials to be welded and the tendency for brittle intermetallic compounds (IMCs) to form in the fusion zone (Qiu et al., 2009). Furthermore, the heat effect from fusion welding also deteriorates the properties of the base material around the weld (Hwang and Chou, 1998). Non-welding techniques, such as fastening coupled with adhesive bonding, provide alternate means of dissimilar joining (Abe et al., 2006; Barnes and Pashby, 2000; Mori et al., 2006). However, fasteners add weight and cost. In high volume production this inhibits the widespread use of fasteners. Solid-state welding techniques such as friction-stir welding and related techniques such as refill friction stir spot welding can join some combinations of dissimilar materials without copious IMCs (Jana et al., 2010; Watanabe et al., 2006; Fukada et al., 2013), but cycle time and geometrical constraints have also limited their application. While many of these techniques have their merits, there is still need for a breakthrough technique that can perform dissimilar metal joining effectively, economically, and flexibly.

In this study, welding was carried out using vaporizing foil actuator welding (VFAW) (Vivek et al., 2013), a solid-state impact welding technique. VFAW is similar to explosion welding (EXW) (Acarer & Demir, 2008) and magnetic pulse welding (MPW) (Manogaran et al., 2014) in that it welds materials in solid-state by means of a high-speed oblique impact that takes place between the two materials being welded. Such an impact forces the oxide films on the colliding surfaces to be ejected in the form of a jet (Abrahamson, 1961), and brings nascent surfaces into atomistically intimate contact, thus creating a metallurgical bond (Mårtensson and Schweitz, 1985). Since impact welding does not require heating and melting, IMC formation can largely be avoided, given appropriate welding parameters. However, in the case where impact energy is excessive, the severe shear deformation near the weld interface may give rise to localized heating and even melting, leading to the formation of IMCs. In many cases, a small amount of IMCs along the weld interface is acceptable, as long as they are thin and discontinuous. It also matters what types of IMCs are present, since some IMCs are more brittle than others (Lei et al., 2015). In any case, understanding the nature and distribution of IMCs present at the weld interface is critical to predicting the properties of the joint.

Another concern with dissimilar joining is galvanic corrosion. In the case of Al/Fe joining, which is highly sought after in the automotive industry, aluminium is often the more anodic element of the pair and is corroded at an accelerated rate. One way to mitigate galvanic corrosion is to create a graded transition joint, where the corrosion potential changes gradually, but this is often difficult or expensive to achieve. A more common way is to use insulating layers to either separate the galvanic couple or isolate the entire joint area from corrosive environment. The former can be done with non-welding techniques, such as fastening coupled with adhesive bonding, or by augmenting the weld with a coating, seal or gasket. Where welding is employed, only the latter strategy against galvanic corrosion is available, typically in the form of a passivation coating, such as e-coating.

The success of impact welding largely depends on two parameters: the angle and speed of the impact. In order to obtain a successful impact weld, these two parameters must fall within some optimal range, known as the welding window (Mousavi and Sartangi 2009). In VFAW, welding typically takes place along the outer perimeter of the active area of the foil actuator, forming a race-track-shaped weld zone (**Fig. 1(a)**). Wavy features can be found at the weld interface, and they are characteristic of impact welding processes (Ben-Artzy et al., 2008). The center of the impacted area is typically not welded because the impact angle is too low. The bonded flyer has a complex shape due to the initial standoff (**Fig. 1(b)**).

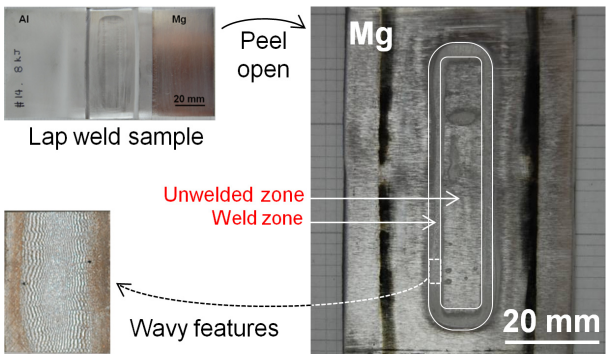

(a)

(b)

***Figure 1**: (a) Top view of a peeled VFAW joint. (b) Side cross section of a VFAW joint*

2 Experimental Method

In this study, four Al/Fe combinations were welded using VFAW:

- AA5052/JAC980
- AA5052/JSC1500
- AA6111-T4/JAC980
- AA6111-T4/JSC1500

The four combinations include two wrought aluminium alloys (AA5052 and AA6111-T4) and two high strength steels (JAC980 and JSC1500). All four alloys are of high interest in the automotive industry. JAC980 is dual-phase steel with minimum ultimate tensile strength of 980 MPa, and JSC1500 is boron steel with minimum ultimate tensile strength of 1500 MPa. JAC980 is galvannealed steel, with a zinc coating. JSC1500 was hot-rolled and was covered with mill scale. To provide a study on the joining of base materials, the surface layers of both steels were removed by surface grinding, in the areas

where welding was to take place. About 0.1 to 0.2 mm of material was removed from each steel plate.

The welding event can be characterized by voltage and current traces using an oscilloscope. Flyer velocities were measured in separate experiments using photonic Doppler velocimetry (PDV) (Strand et al., 2006; Vivek et al., 2014). The welded joints were studied by mechanical testing, cross-sectional microscopy, and corrosion testing.

Six weld coupons were made by VFAW, using the same welding parameters: 10 kJ input energy and 1.6 mm standoff. Of the six weld coupons, two were sectioned and mechanically tested in lap-shear. Sectioning was done by water jet, and each coupon yields two samples for testing, each sample measuring about 1/2 inch (12.7 mm) wide. An additional cross-section of the weld interface of each material combination was mounted and polished for metallography, using standard mounting and polishing procedures.

The remaining four weld coupons were subjected to 30 cycles of corrosion testing according to ASTM B-117 (5% NaCl salt spray, 30 °C, 24 hours/cycle). Of the four weld coupons, two were e-coated (by Electro Prime Inc., using POWERCRON® 6000CX) and two were left bare. After corrosion testing, the four coupons were sectioned by water jet and mechanically tested in lap-shear, the same way as first two weld coupons.

Overall, twelve test cases were explored (four material combinations and three test conditions: as-welded, corrosion-tested with e-coating, and corrosion-tested without e-coating). Four test samples were obtained for each case. A total of 48 samples were tested.

For additional corrosion characterization, the open cell potentials (OCP) of the base materials were measured individually in 5% NaCl solution at room temperature. To prepare for the tests, sheet metals were polished to 1200 fine grit. The Al alloys were polished in ethanol instead of water for 800 grit and beyond. Sample area was 1 cm^2. Corrosion pits were measured using optical profilometry.

3 Results and Discussion

3.1 Flyer Velocity Traces

Flyer velocity traces are shown in **Fig. 2**. The 1.6 mm standoff distance is taken to represent the impact velocity. The impact velocities were 700 m/s for the AA5052 flyer and 727 m/s for the AA6111-T4 flyer.

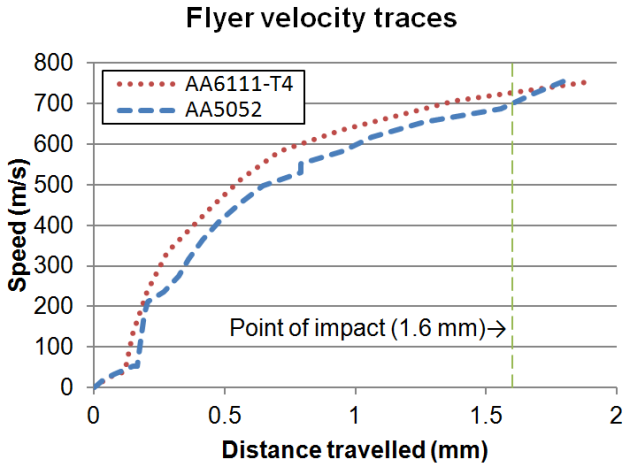

***Figure 2**: Flyer velocity traces*

3.2 Mechanical Testing

Mechanical testing results are summarized in **Fig. 3**. Majority (38 out of 48) of the test samples, both before or after corrosion testing, failed in the base aluminium, indicating that the weld, when loaded in lap-shear, was stronger than at least one of the base materials. Failure most frequently occurs near the bent area of the flyer. Of the ten samples that failed along the weld, seven failed prior to mechanical testing, perhaps due to weld defects or damage during sectioning and handing. Only three samples failed along the weld interface during mechanical testing.

After 30 cycles of B-117 corrosion testing, the e-coated AA5052/JAC980 samples only degraded 2.4% in strength. On the other hand, the e-coated AA5052/JSC1500 samples experienced an 18.4% decrease in strength, with two samples failing in the weld and two samples failing in the base Al. If one only counts the samples that failed in the base Al, however, the strength degradation was only 3.4%. The e-coated AA6111-T4 samples suffered more significant strength reduction than their AA5052 counterparts (20.0% for AA6111-T4/JAC980 and 34.0% for AA6111-T4/JSC1500). The uncoated samples underwent more significant strength reduction after corrosion testing: 36.8% reduction for AA5052/JAC980, 35.4% reduction for AA5052/JSC1500, 49.3% reduction for AA6111-T4/JAC980, and 47.2% reduction for AA6111-T4/JSC1500. Nonetheless, in both e-coated and uncoated conditions, majority of the samples still failed in base aluminium, rather than along the weld. This indicates that the strength degradation was largely due to deterioration of the base materials, not of the weld. No significant overall thickness reduction of base materials was detected, but localized corrosion pits did reduce the local cross section and can provide stress concentration.

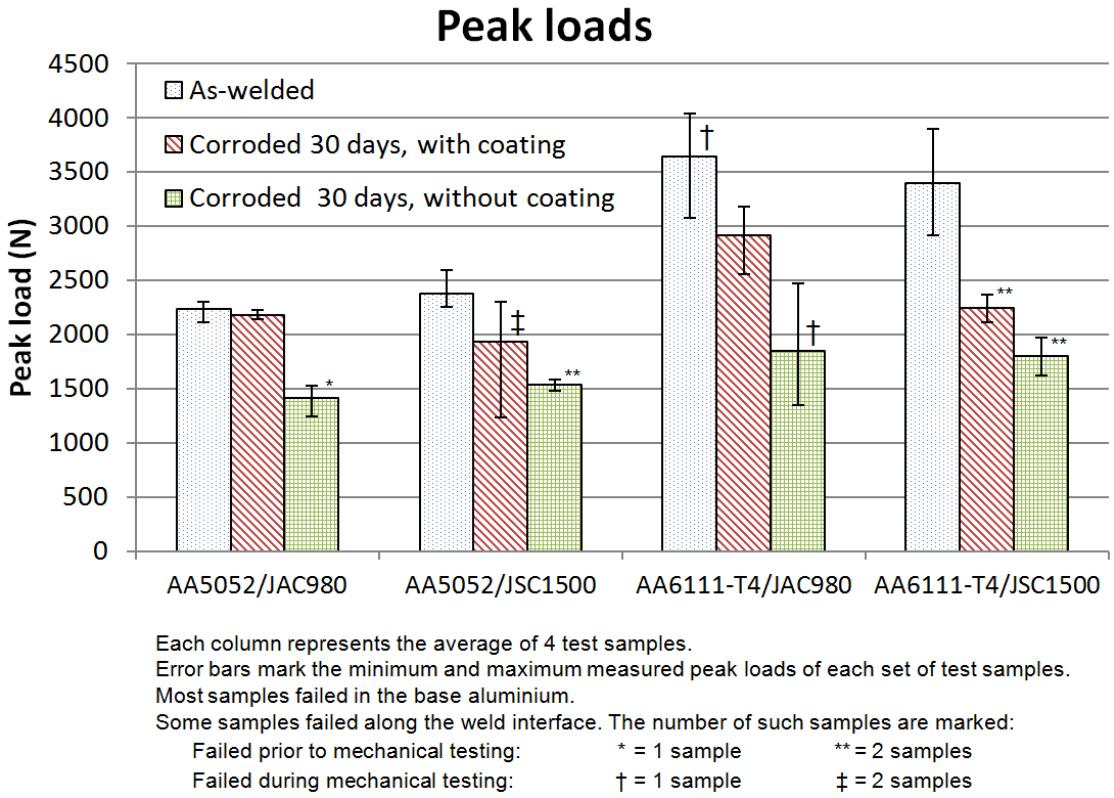

***Figure 3**: Peak loads at various test conditions*

3.3 Metallography

Wavy features, which are common to impact welding (Cowan et al., 1971), could be seen at the weld interfaces. The width of each welded area was about 2 mm, viewed from this cross section. The severe shear deformation near the weld interface can sometimes give rise to significant heating and mixing, which can lead to formation of intermediate phases, such as IMCs, especially at the trunks and tails of the waves, where mixing and heating are the most significant (Bahrani et al., 1967). Intermediate phases were present at the interfaces of all four welded material combinations (**Fig. 4**), but all four combinations also have IMC-free regions, which may account for most of the weld's toughness.

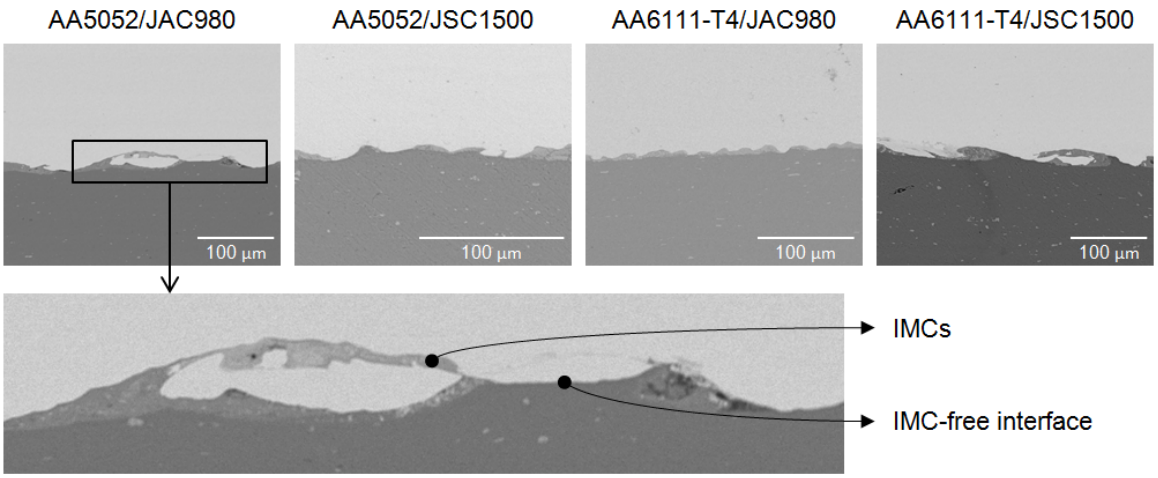

***Figure 4**: Backscattered electron images of weld cross sections*

3.4 Corrosion Characterization

Open cell potentials of the base materials are summarized in **Table 1**. Generally, aluminium is expected to be more anodic than steel and susceptible to galvanic corrosion when joined to steel. However, it turned out that the four materials had very similar OCP's, and in some cases, the steel was found to be more anodic than the aluminium. The largest difference in OCP was the one between JAC980 and AA6111-T4, with a magnitude of 0.060 V, which is rather small, for most applications. This is consistent with the fact that no significant galvanic corrosion was observed during corrosion testing of the weld coupons.

Metal	OCP (V SCE)
AA5052	-0.746
AA6111-T4	-0.698
JAC980	-0.758
JSC1500	-0.690

***Table 1:** Open cell potentials of base metals*

Corrosion pits were found near the bent area of the flyer (**Fig. 5**). This could be due to accumulation of salt and moisture in the crevice in this area. In addition, jetted materials from the welding process also could have accumulated here. Jetted materials are a mixture of particles from both base materials, their oxides, and other contaminants. As such, this mixture of materials could affect the corrosion characteristics in the areas where they accumulate. Once corrosion took place and localized corrosion pits formed, they acted as stress concentrators which weakened the base material in mechanical testing.

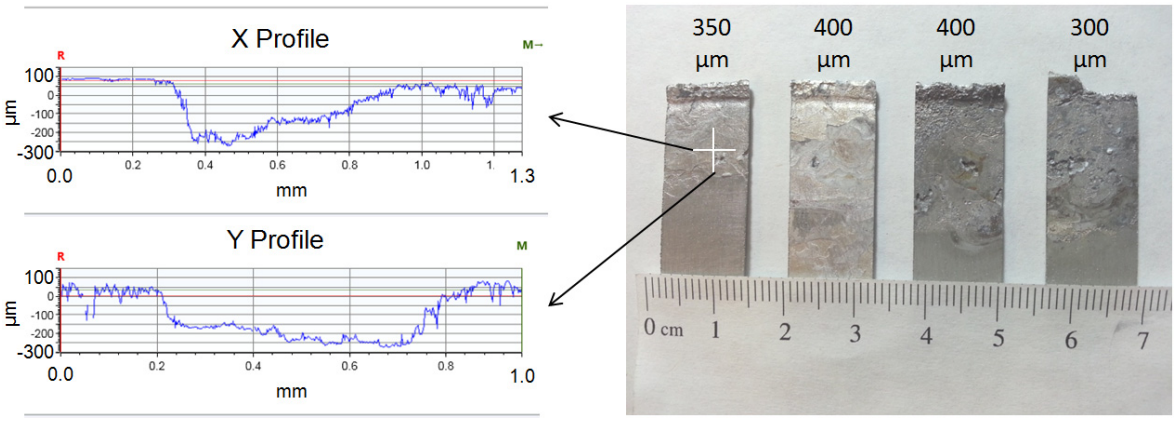

***Figure 5**: Corroded uncoated aluminium, extracted from the four weld combinations (ordered from left to right): AA5052/JAC980, AA5052/JSC1500, AA6111-T4/JAC980, AA6111-T4/JSC1500. Approximate depths of representative corrosion pits are indicated above each sample.*

Conclusion

Four Al/Fe combinations of automotive aluminium and steel alloys were welded successfully using VFAW. In lap-shear testing, the majority of the test samples failed in the base aluminium, for all three test conditions (as-welded, corrosion tested with e-coating, and corrosion-tested without e-coating). This indicates that the shear strength of the weld exceeds the material strength of the base aluminium. Failure tended to occur in the bent area of the flyer. OCP's of all four materials were found to be very close to one another, and thus the effect of galvanic corrosion was not significant during corrosion testing of weld coupons. Pitting corrosion in the base aluminium near the bent area of the flyer weakened the materials, but the adverse effects of corrosion were mitigated by e-coating. In the case of corrosion testing AA5052/JAC980, the e-coated samples only lost 2.4% of their strength, while the uncoated samples lost 18.4%. Therefore effective isolation of the welded joint from the corrosive environment will be an important strategy against corrosion of dissimilar joints. This suggests that this process can be developed to join aluminium and steel with useful and predictable engineering properties and durability.

Acknowledgement

The authors are thankful for sponsorship from the U.S. Department of Energy's Vehicle Technologies Office under grant no. DE-EE0006451. Special thanks go to Honda Motor Company for supplying JAC980 and JSC1500 used in this work. Many thanks go to Jichao Li, Benjamin Hanna, and Zhicao Feng for assisting with corrosion characterizations, and to Taylor Dittrich for acquiring SEM images and profilometry measurements.

References

Abe, Y., Kato, T., Mori, K., 2006. Joinability of aluminium alloy and mild steel sheets by self piercing rivet. Journal of Materials Processing Technology, 177, 417–421. doi:10.1016/j.jmatprotec.2006.04.029

Abrahamson, G., 1961. Permanent periodic surface deformations due to a traveling jet. Journal of Applied Mechanics. Retrieved from http://appliedmechanics.asmedigitalcollection.asme.org/article.aspx?articleid=1394803

Acarer, M., Demir, B., 2008. An investigation of mechanical and metallurgical properties of explosive welded aluminum–dual phase steel. Materials Letters, 62(25), 4158–4160. doi:10.1016/j.matlet.2008.05.060

Bahrani, A. S., Black, T. J., Crossland, B., 1967. The mechanics of wave formation in explosive welding. Proceedings of the Royal Society of London. Series A. Mathematical and Physical Sciences, 296(1445), 123–136. Retrieved from http://rspa.royalsocietypublishing.org/content/296/1445/123.short

Barnes, T. A., Pashby, I. R., 2000. Joining techniques for aluminum spaceframes used in automobiles. Part II - adhesive bonding and mechanical fasteners. Journal of Materials Processing Technology, 99, 72–79. doi:10.1016/S0924-0136(99)00361-1

Ben-Artzy, A., Stern, A., Frage, N., Shribman, V., 2008. Interface phenomena in aluminium–magnesium magnetic pulse welding. Science and Technology of Welding and Joining, 13(4), 402–408. doi:10.1179/174329308X300136

Cowan, G. R., Bergmann, O. R., Holtzman, A. H., 1971. Mechanism of bond zone wave formation in explosion-clad metals. Metallurgical and Materials Transactions B, 2(November), 3145–3155. Retrieved from http://link.springer.com/article/10.1007/BF02814967

Fukada, S., Ohashi, R., Fujimoto, M., Okada, H., 2013. Refill friction stir spot welding of dissimilar materials consisting of A6061 and hot dip zinc-coated steel sheets. Proceedings of the 1st International Joint Symposium on Joining and Welding (pp. 183–187). Woodhead Publishing Limited. doi:http://dx.doi.org/10.1533/978-1-78242-164-1.183

Hwang, R. Y., Chou, C. P., 1998. The Study on Microstructural and Mechanical Properties of Weld Heat Affected Zone of 7075-T651 Aluminum Alloy, 38(2), 215–221.

Jana, S., Hovanski, Y., Grant, G. J., 2010. Friction stir lap welding of magnesium alloy to steel: A preliminary investigation. Metallurgical and Materials Transactions A: Physical Metallurgy and Materials Science, 41(December), 3173–3182. doi:10.1007/s11661-010-0399-8

Joost, W. J., 2012. Reducing Vehicle Weight and Improving U.S. Energy Efficiency Using Integrated Computational Materials Engineering. Jom, 64(9). doi:10.1007/s11837-012-0424-z

Lei, H., Li, Y., Carlson, B. E., Lin, Z., 2015. Cold Metal Transfer Spot Joining of AA6061-T6 to Galvanized DP590 Under Different Modes. Journal of

Manufacturing Science and Engineering, 137(NOVEMBER), 051028. doi:10.1115/1.4029093

Manogaran, A. P., Manoharan, P., Priem, D., Marya, S., Racineux, G., 2014. Magnetic pulse spot welding of bimetals. Journal of Materials Processing Technology, 214(6), 1236–1244. doi:10.1016/j.jmatprotec.2014.01.007

Mårtensson, N., Schweitz, J., 1985. Fundamental aspects of formation and stability of explosive welds. Metallurgical Transactions A, 16(May), 841–852. Retrieved from http://link.springer.com/article/10.1007/BF02814835

Mori, K., Kato, T., Abe, Y., Ravshanbek, Y., 2006. Plastic joining of ultra high strength steel and aluminium alloy sheets by self piercing rivet. CIRP Annals - Manufacturing Technology, 55(2), 283–286. doi:10.1016/S0007-8506(07)60417-X

Mousavi, S. A. A. A., Sartangi, P. F., 2009. Experimental investigation of explosive welding of cp-titanium/AISI 304 stainless steel. Materials Design, 30(3), 459–468. doi:10.1016/j.matdes.2008.06.016

Qiu, R., Iwamoto, C., Satonaka, S., 2009. Interfacial microstructure and strength of steel/aluminum alloy joints welded by resistance spot welding with cover plate. Journal of Materials Processing Technology, 209, 4186–4193. doi:10.1016/j.jmatprotec.2008.11.003

Strand, O. T., Goosman, D. R., Martinez, C., Whitworth, T. L., Kuhlow, W. W., 2006. Compact system for high-speed velocimetry using heterodyne techniques. Review of Scientific Instruments, 77(8), 083108. doi:10.1063/1.2336749

Vivek, A., Hansen, S. R., Daehn, G. S., 2014. High strain rate metalworking with vaporizing foil actuator: control of flyer velocity by varying input energy and foil thickness. The Review of Scientific Instruments, 85(7), 075101. doi:10.1063/1.4884647

Vivek, A., Hansen, S. R., Liu, B. C., Daehn, G. S., 2013. Vaporizing foil actuator: A tool for collision welding. Journal of Materials Processing Technology, 213(12), 2304–2311. doi:10.1016/j.jmatprotec.2013.07.006

Watanabe, T., Takayama, H., Yanagisawa, A., 2006. Joining of aluminum alloy to steel by friction stir welding. Journal of Materials Processing Technology, 178, 342–349. doi:10.1016/j.jmatprotec.2006.04.117